Surface & Coatings Technology 441 (2022) 128587



Contents lists available at ScienceDirect

Surface & Coatings Technology

journal homepage: www.elsevier.com/locate/surfcoat





Tribocorrosion properties of plasma nitrided, Ti-DLC coated and duplex surface treated AISI 316L stainless steel

Y. Uzun

Ataturk University, Faculty of Engineering, Department of Mechanical Engineering, Erzurum, Turkey

ARTICLE INFO

Keywords:
316L stainless-steel
Plasma nitriding
Ti-DLC coating
Duplex surface treatment
Tribocorrosion

ABSTRACT

In this study, the tribocorrosion behavior of untreated, plasma nitrided (450 °C–4 h), Ti-DLC coated and duplex treated (Ti-DLC coating after nitriding) AISI 316L stainless-steel were investigated. The plasma nitriding process was carried out in a gas mixture of 80 % H_2 and 20 % N_2 at 450 °C for 4 h. A titanium (Ti) interlayer was coated on the substrate for Ti-DLC coating. Then, a diamond-like carbon (DLC) film was grown on the Ti interlayer. As a result of the study, it was determined that the damage caused by the wear mechanism was much more than the corrosive effects. In general, thanks to the layers formed on the surface, the wear and tribocorrosion performance of the treated samples increased compared to the untreated sample. It was observed that the best tribocorrosion resistance among the treated surfaces was obtained in the duplex surface-treated sample.

1. Introduction

AISI 316L stainless steel are often used in different applications where excellent corrosion resistance, non-magnetic properties, high ductility and biocompatibility are required [1,2]. However, it shows poor mechanical properties when they are used in places where severe wear and corrosion conditions, such as human body. Additionally, in many studies, it was determined that elements such as Ni and Cr in the structure of AISI 316L stainless steel are released into the body due to corrosion in the body environment [3,4]. In order to minimize the harmful effects of this release, special surface modification processes are applied to AISI 316L stainless steel [5]. With these surface treatments, the structural, tribological and electrochemical properties of the material are improved. Plasma nitriding, Ti-DLC coating and duplex surface treatments used in this study are often used to impart extraordinary properties to materials such as high hardness, low coefficient of friction and high wear-corrosion resistance under different operating conditions [6].

Among the known surface modification techniques, plasma nitriding is known to be one of the most preferred methods. In this process, the nitrogen (N) atom is diffused into the inner parts of the material with a decreasing concentration in the plasma environment. Thus, a hard diffusion layer are obtained. Also, sputtering effect during nitriding provides a compound layer, which consist of nitrides. Studies in the literature shown that the surface hardness of the modified substrate generally increases with increasing process time and temperature. Additionally, it was reported that nitriding at 450 °C provides the best corrosion resistance. On the other hand, it is possible to see in these studies that an increase in temperature from 450 °C to 600 °C adversely affects the corrosion resistance of stainless-steel in a NaCl solution [7–12]. Also, another study stated that nitriding of AISI 316L at 450 °C up to 25 % N_2 rate did not form CrN even if it was applied for long nitriding periods [13].

DLC is the abbreviation of diamond-like carbon. With a DLC coating, materials are given properties such as high hardness, low friction coefficient and excellent wear and corrosion resistance under intense working conditions [14,15]. However, the high Young's modulus of DLC films and their high film stresses relative to the substrate can cause these films to deteriorate suddenly. The pre-treatment of materials prior to DLC coating can prevent this situation. In general, surface treatments that involve the application of multiple treatments are called duplex surface treatments. Within the scope of this study, the nitriding process and DLC film coating process on substrate as duplex surface treatment are performed one after the other. Here, plasma nitriding is performed as a pre-treatment before DLC film coating. In this process, the DLC film coating on the upper surface with the N content that diffuses inward from the upper surface of the material and gradually decreases is called the compound layer. This layered structure provides a smooth transition of hardness between the DLC film and the substrate, as well as a high load carrying capacity. Thus, thanks to duplex treatment processes involving DLC films, some tribological properties are provided to materials [6].

E-mail address: yakup.uzun@atauni.edu.tr.

https://doi.org/10.1016/j.surfcoat.2022.128587
Received 28 March 2022; Received in revised form 25 May 2022; Accepted 31 May 2022
Available online 6 June 2022
0257-8972/© 2022 Elsevier B.V. All rights reserved.

Table 1
Chemical composition of AISI 316L stainless-steel (wt%).

Element	C	Cr	Ni	Mo	Mn	Cu	N	Fe
Wt%	0.02	16.9	11.2	2.1	1.47	0.03	0.06	Balance

In the literature, there are many studies investigating the mechanical and tribological properties of surfaces treated with plasma nitriding, DLC coating and duplex surface treatment. In these studies, it was seen that the electrochemical corrosion and mechanical wear properties of materials can be improved as a result of the application of plasma nitriding, DLC coating and duplex surface treatments alone or together [16–18]. Morten et al. investigated the erosion, corrosion and tribocorrosion behavior of surface-modified AISI 316L stainless steel in salt water [19]. They reported that the DLC film coating and low temperature nitriding process significantly reduced the amount of erosion-corrosion of the stainless steel in a corrosive environment. Likewise, Azzi et al. investigated the wear and corrosion behavior of AISI 316L stainless steel with DLC coating in Ringer's solution and reported that the protective properties of the DLC coating were not affected by friction and the structure showed excellent tribocorrosion properties [20]. Bayón et al. evaluated the corrosion and tribocorrosion responses of three different Ti-DLC coatings with different compositions, obtained by physical vapor deposition (PVD) on the surfaces of biomedical grade Ti6Al4V samples, in simulated body fluid (SBF). As a result of their study, the authors reported that the coatings with high carbon content had excellent tribocorrosion responses [21]. Guo et al. studied the tribocorrosion performance of the CoCrMo alloy by applying different surface modifications such as plasma nitriding and DLC coating at different process temperatures with PVD method [22]. As a result, they reported that the DLC coated samples presented a low anodic corrosion current due to the chemical inertness of carbon. Magdalena et al. applied TiN coating using the CAE-PVD (Cathodic Arc Evaporation-PVD) method and DLC film coating with PACVD (Plasma Assisted Chemical Vapor Deposition) method to improve the tribological properties of AISI 316LVM medical grade stainless steel [23]. They observed extremely different wear and cracking patterns for the two thin films. In scratch tests, they observed a six-stage deformation regime in the DLC coating, while four main cracking stages were recorded for the TiN coating. Based on their results, they reported that the TiN coating provided better adhesion to the substrate than the DLC coating in the wear tests, despite its poor performance in the scratch tests.

Although there are many different studies dealing with the corrosion, wear and tribocorrosion properties of surface treated AISI 316L stainless steel separately, any studies was not performed to compare the tribocorrosion performance of plasma nitrided, DLC coated and duplex surface treated AISI 316L stainless steel. In this context, this study was carried out to investigate the tribocorrosion behavior of plasma nitrided, DLC-coated and duplex surface treated (Ti-DLC coating on plasma nitriding) AISI 316L stainless steel in a simulated body fluid (SBF) environment.

2. Experimental details

In this study, AISI 316L austenitic stainless-steel, whose chemical composition is given in Table 1, was used. Steel samples with a diameter of 15 mm were cut with 5 mm thickness and mechanically polished with 80–1200 sandpapers, respectively. The samples were then polished further with alumina powders with grain sizes of 0.3–0.5 μm. The prepared samples were cleaned with ethanol to get rid of the abraded particles.

Afterwards, the samples were placed in the plasma nitriding chamber, which is illustrated in Fig. 1 and they were vacuumed up to 3 Pa pressure by vacuum pump. Prior to plasma nitriding, the samples were hydrogen sputtered for 20 min at a voltage between 400 and 500 V and a pressure of 5×10^2 Pa to remove contaminations from the sample surfaces. Then, the plasma nitriding process was carried out in a gas mixture of 80 % H_2 and 20 % N_2 at 450 °C for 4 h. The temperature was

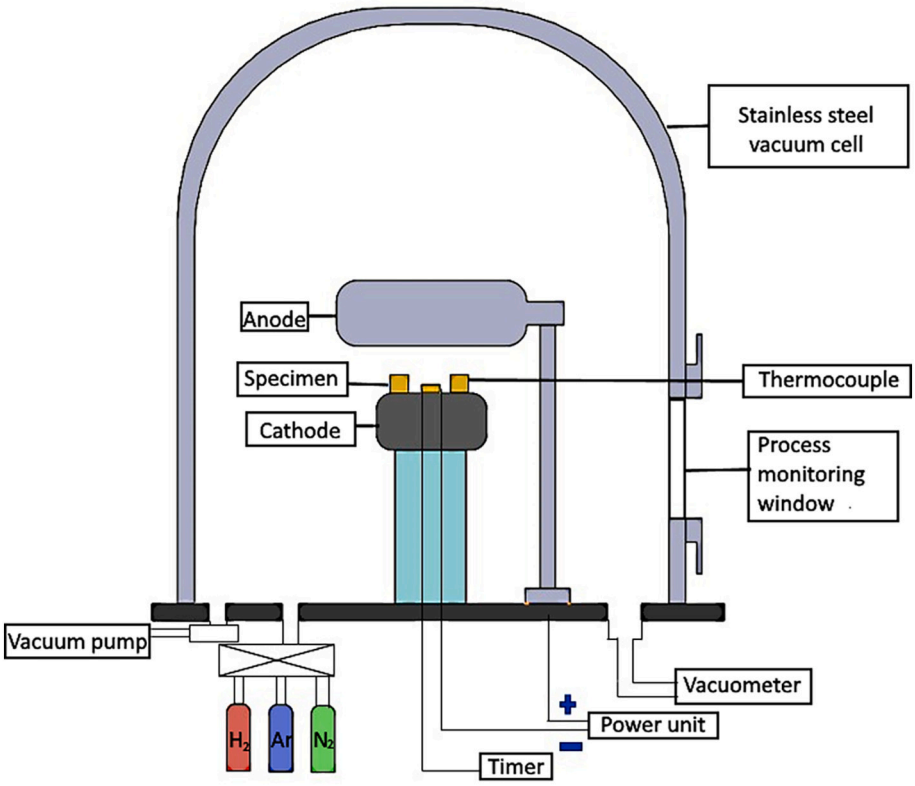


Fig. 1. Plasma nitriding testing apparatus.

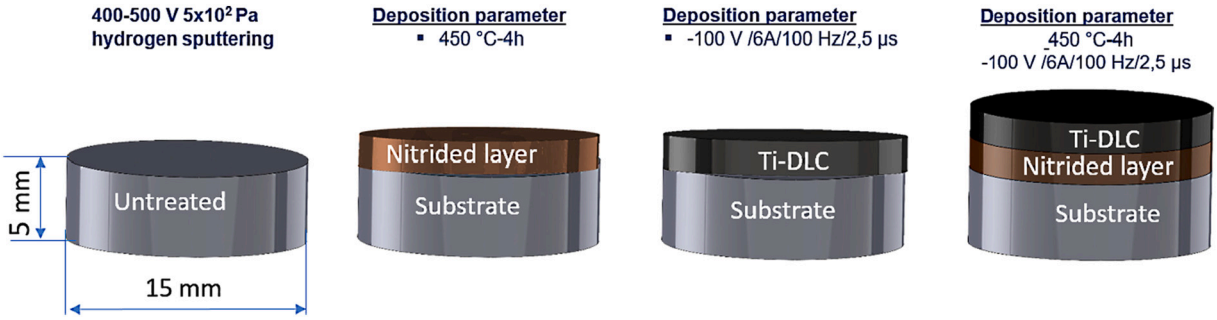


Fig. 2. The deposition parameters of plasma nitrided, DLC coated and duplex treated samples.

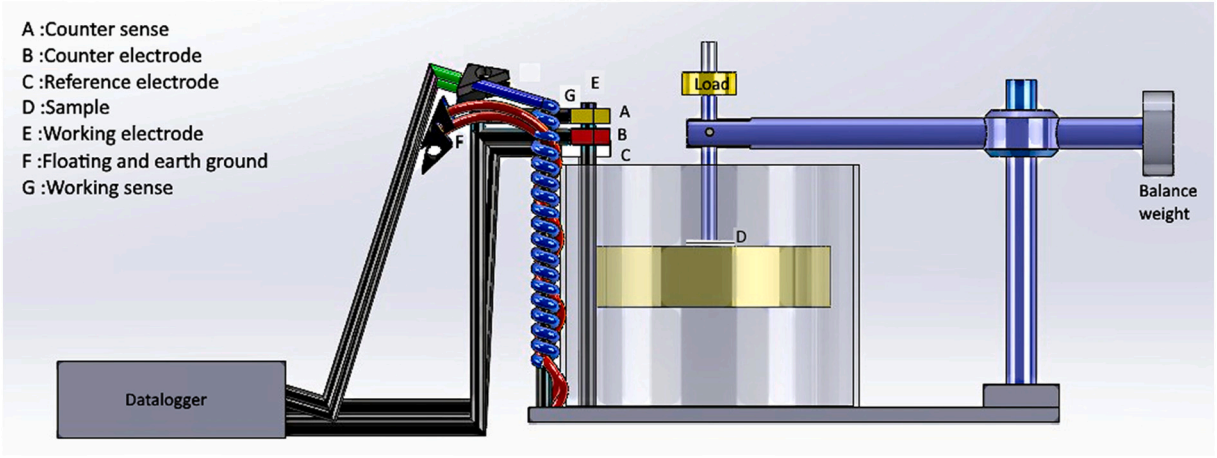


Fig. 3. Tribocorrosion test setup.

Table 2
Tribocorrosion parameters.

Normal load	5 N
Relative wear distance	96 m
Stroke length	8 mm
Sliding velocity	16 mm/s
Alumina ball diameter	6 mm
OCP Total Time	6000 s
Electrolyte	SBF solution
Temperature	22 °C
Reference electrode	Ag/AgCl
Counter electrode	Graphite

Table 3
Preparation of SBF for pH 7.25, 1 l [24].

No	Reactive	Quantity
1	NaCl	7.966 g
2	$NaHCO_3$	0.350 g
3	KCl	0.224 g
4	$K2HPO_4•3H_2O$	0.228 g
5	$MgCl_2•6H_2O$	0.305 g
6	1 kmol/m^3 HCl (35.4 % HCl 87.28 ml, diluted)	40 cm^3
7	$CaCl_2$	0.278 g
8	Na_2SO_4	0.071 g
9	$(CH_2OH)_3CNH_2$	6.057
10	1 kmol/m^3 HCl	for pH adjustment, appropriate amount was used

measured with a thermocouple placed on the sample holder cathode during the process.

After plasma nitriding, Ti-DLC coating processes were performed. Ti-DLC coating processes were carried out with VAKSIS PVD-MT/2M 2T magnetron sputtering system. A 50.8 mm carbon target was used for the coating. The distance between the target and the base materials was 9 cm. In order to obtain more homogeneous films, the substrates were rotated at 5 rpm. The front (base) pressure of the vacuum chamber (chamber) before coating was approximately 2×10^3 Pa. After reaching the desired vacuum value, Ar gas was given to the chamber and the ambient working pressure was fixed at its value. After this, ion cleaning was performed to get rid of contaminations. In order to provide better contact on the base material, reduce residual stresses at the interface between the film and the substrate and provide better adhesion by removing the oxide layer on the surface of the base material, a Ti interlayer was coated on substrate. After all these processes, a DLC film was grown onto the Ti interlayer. DLC coating process was carried out according to the conditions determined in the experiment plan (−100 V base material bias voltage, 6A Ti target current, 100 Hz frequency, 2.5 µs pulse duration). DLC films were grown at 20 sccm argon gas flow, under 0.27 Pa process pressure and 150 W DC power and argon gas was used for the ionization process. When the coating period was over, the current and voltage were cut off and the samples were left to cool. Thus, four groups of specimens were obtained: untreated, plasma nitrided, Ti-DLC coated and duplex treated (plasma nitrided + Ti DLC coated samples). The parameters for obtaining the samples are illustrated in Fig. 2.

In order to determine the tribocorrosion properties of the samples, corrosion and wear tests were carried out by using the relevant devices simultaneously. The tribocorrosion test device is shown in Fig. 3, and the values of the parameters used in the tribocorrosion test are given in Table 2. In the tribocorrosion tests, a sample holder was used, and it was known that the surface areas of the samples in contact with the solution were 2 cm^2 in this holder. During the test, first, Open Circuit Potential

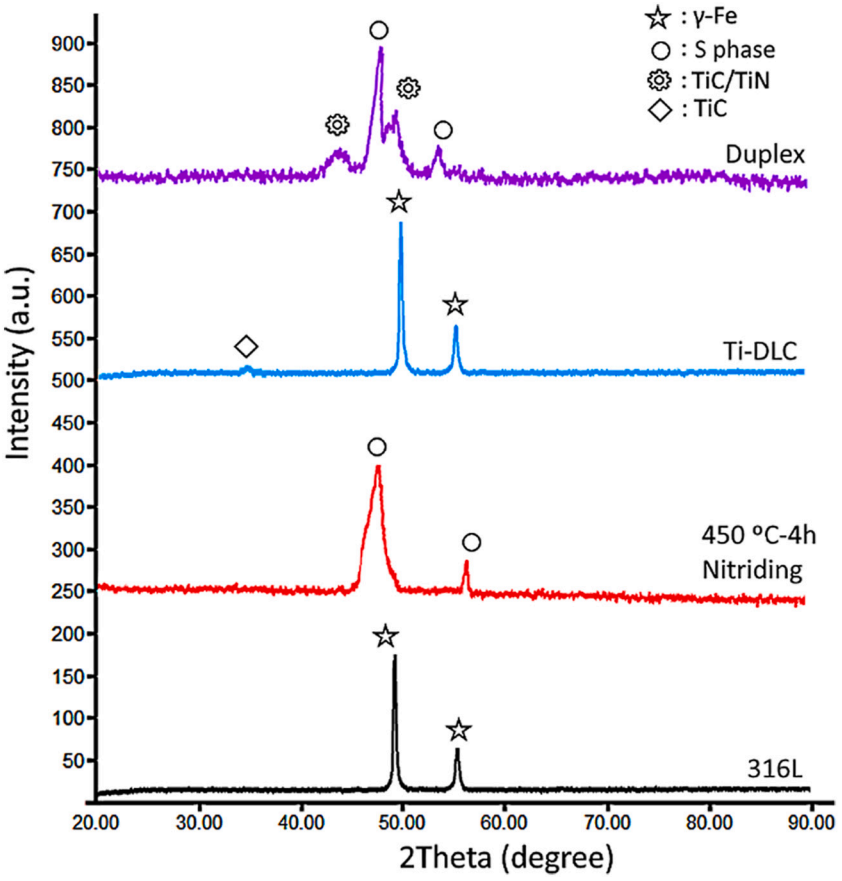


Fig. 4. XRD plots of untreated, plasma nitrided, Ti-DLC coated and duplex surface treated samples.

(OCP) measurements of the samples were made for 4000 s with load. In the tribocorrosion tests, a 6-mm-diameter alumina (Al_2O_3) ball was used for wear, the wear frequency was adjusted to 1 Hz and the wear track length was set as 8 mm. Tribocorrosion tests were performed at room temperature using a flat ball tribometer (UMT-2, Bruker instrument) connected to a three-electrode chemical cell (Fig. 3) in an SBF solution (the chemical composition of SBF is given in Table 3) in which the samples were immersed. The tribocorrosion tests were performed according to the experimental parameters shown in Table 2 and by following the ASTM G119-09 procedure.

The tribocorrosion behavior of the surfaces of the untreated, plasma nitrided, Ti-DLC coated and duplex surface treated (Ti-DLC coating after plasma nitriding) 316L stainless steel samples were tested in the SBF solution. In these ambient conditions, open circuit potential (OCP) measurements were made for 4000 s, and the reading was taken. Before starting the wear tests, OCP measurements were taken for 1000 s and then, the wear process was carried out for 4000 s. OCP measurements were made again without wear for 1000 s immediately after the wear process was finished. Thus, the experiment was completed. During the experiments, the friction coefficient was given automatically by the device, and the surface roughness was determined using the profilometer before and after the experiment. After the tribocorrosion tests, the data were analyzed with the Gamry Echem Analyst software. All tests and measurements were repeated at least three times. After the tests, mean values and standard deviations were calculated. The wear rate of the coating was determined by the following equations (Eq. (1) and Eq. (2)):

$$Wear\ rate\ of\ the\ coating = \frac{(Wear\ volume)}{(Applied\ load^{*}Wear\ distance)} \quad (1)$$

$$Wear\ distance = Circumference\ of\ the\ wear\ track^{*}Rotational\ speed^{*}Wear\ time \quad (2)$$

Phase identification of the samples was performed using an XRD-GNR-Explorer X-ray diffraction unit with a Co-Kα (λ = 1.7903 Å) source at 40 kV and 30 mA using a 2θ scale from 20° to 90°. In this study, structural characterization of DLC and duplex materials was investigated using WITec alpha 300 R Micro-Raman Spectroscopy. The measurements were obtained with a laser with a wavelength of 532 nm. The laser power is used at 3 mW to reduce the effects of annealing or heating caused by the laser. Scanning Electron Microscopy (SEM FEI-Quanta 250) was used for analyzing cross-sections and worn surfaces. For sectional SEM images, the samples were split by precision cutting after cold bakelite treatment. Then, the sections of the samples in bakelite were sanded to 80–1200 mesh. Afterwards, cleaning was performed with methanol. In order to remove the contaminations formed after coating for surface SEM images, the surface was cleaned with methanol in a magnetic stirrer for 15 min and they were dried. The roughness and wear track morphology (width and depth of the tracks) of the tested surfaces were examined by a 3D surface profilometer (Bruker Contour GT-K1) after the tribocorrosion tests.

3. Results and discussion

3.1. Characterization of samples

The XRD plots of the untreated, plasma nitrided, Ti-DLC-coated and duplex surface treated AISI 316L stainless steel samples are given in Fig. 4. According to the chosen nitriding parameters, s-phase were formed on the material surface. In the sample which was directly coated with Ti-DLC on 316L stainless-steel without nitriding, the TiC phase was

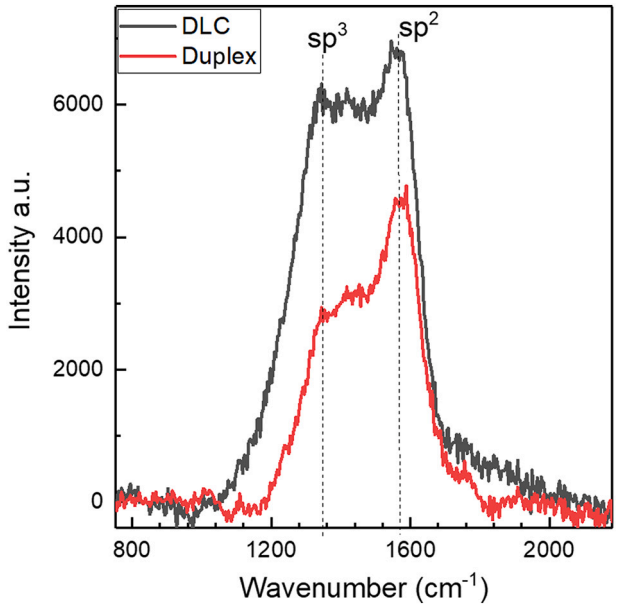


Fig. 5. Raman Spectra of DLC coated and duplex surface treated samples.

observed. The peak of the TiC phase, on the other hand, did not generally have a very strong intensity and exhibited a crystal orientation close to being amorphous. It was observed that s-phase, TiC/TiN phases were formed in the duplex treated sample. The findings obtained as a result of the experiments were identical with other studies in the literature [25]. One of the main goals of improving the surface properties of austenitic stainless steel without impairing its excellent corrosion properties is to increase the surface hardness to withstand extreme wear-inducing conditions. In the nitriding process, it has become important to introduce nitrogen into the austenite matrix without forming the CrN phase, as there is a deterioration in corrosion properties when CrN precipitation occurs. Literature studies showed that nitrided steels with high surface hardness, good wear and corrosion properties can be obtained with the formation of the expanded austenite phase. This can be seen in the plasma nitriding process performed at temperatures below 500 °C. CrN phase does not form in the nitriding process below this temperature [13] Since the experimental condition was applied at 450 °C for 4 h, no CrN phase was formed.

Raman spectrum of Ti-DLC-coated and duplex surface treated AISI 316L stainless steel samples are given in Fig. 5. When the Fig. 5 is examined, it is observed that the D-band is 1349.2 cm^{-1} and the G-band is 1564.4 cm^{-1}. Considering that metal is used in both materials, the Raman vibration found at 1443.7 cm^{-1} can be defined as metal-carbon interaction or defect band. When the Raman spectrum of the duplex coating is examined, a decrease in the intensity of the band, which we consider as metal-carbon, is observed as the excess nitride formation binds the metal.

SEM images of plasma nitrided, Ti-DLC-coated and duplex surface treated AISI 316L stainless steel samples are given in Fig. 6. Based on the cross-section SEM images, while the nitrided layer thickness was measured as approximately 31 μm, Ti-DLC layer's thickness was approximately 6 μm. As it can be observed in Fig. 6, a double layered structure consisting of nitrided layer and DLC is obtained from duplex surface treated sample.

3.2. Tribocorrosion properties

The SEM and 3D profilometer images of the worn surfaces of all samples after the tribocorrosion tests are given in Fig. 7. The calculated wear rates of the samples are given in Table 4. The failure mechanisms and surface morphology the sample surfaces are shown with arrows in the SEM images. As observed in Fig. 7, the damage caused by the wear mechanism was much more than the corrosive effects. Under the OCP conditions, no voltage was applied to the anodic region, so the solution acted as a lubricant here. All samples showed similar morphologies under the OCP conditions. At the beginning of the wear, the stainless steel sample and the Al_2O_3 ball came into direct contact with each other by a two-body mechanism. It is thought that the strong adhesion

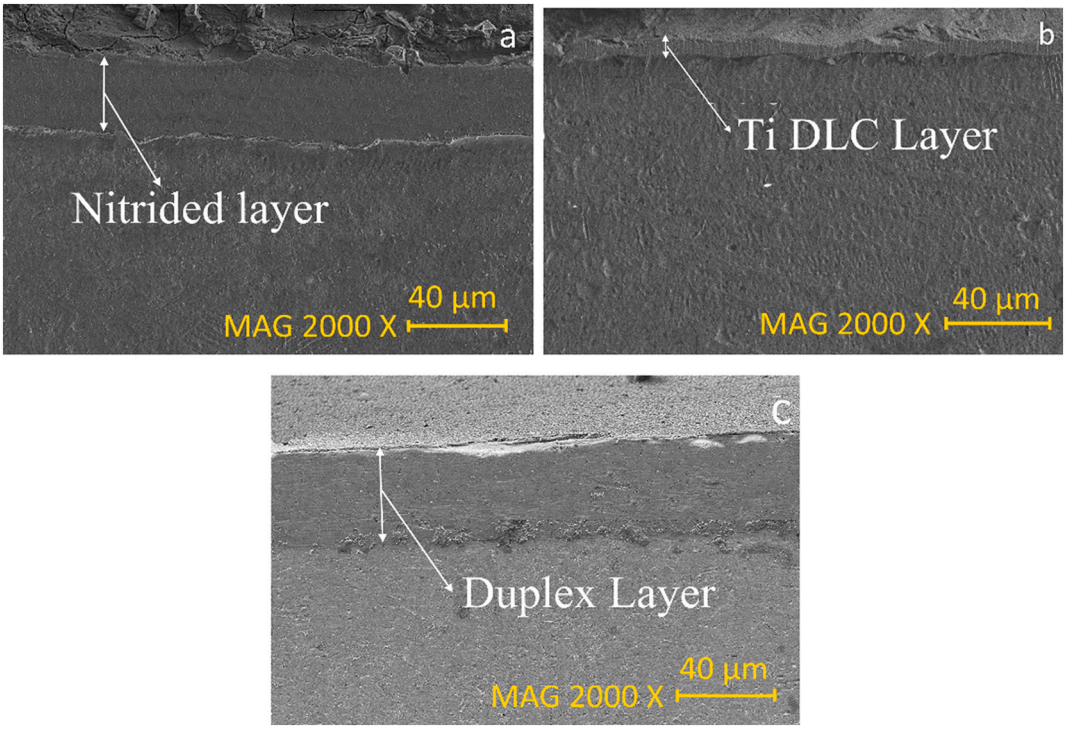


Fig. 6. SEM images of: a) plasma nitrided, b) Ti-DLC-coated and c) duplex surface treated samples.

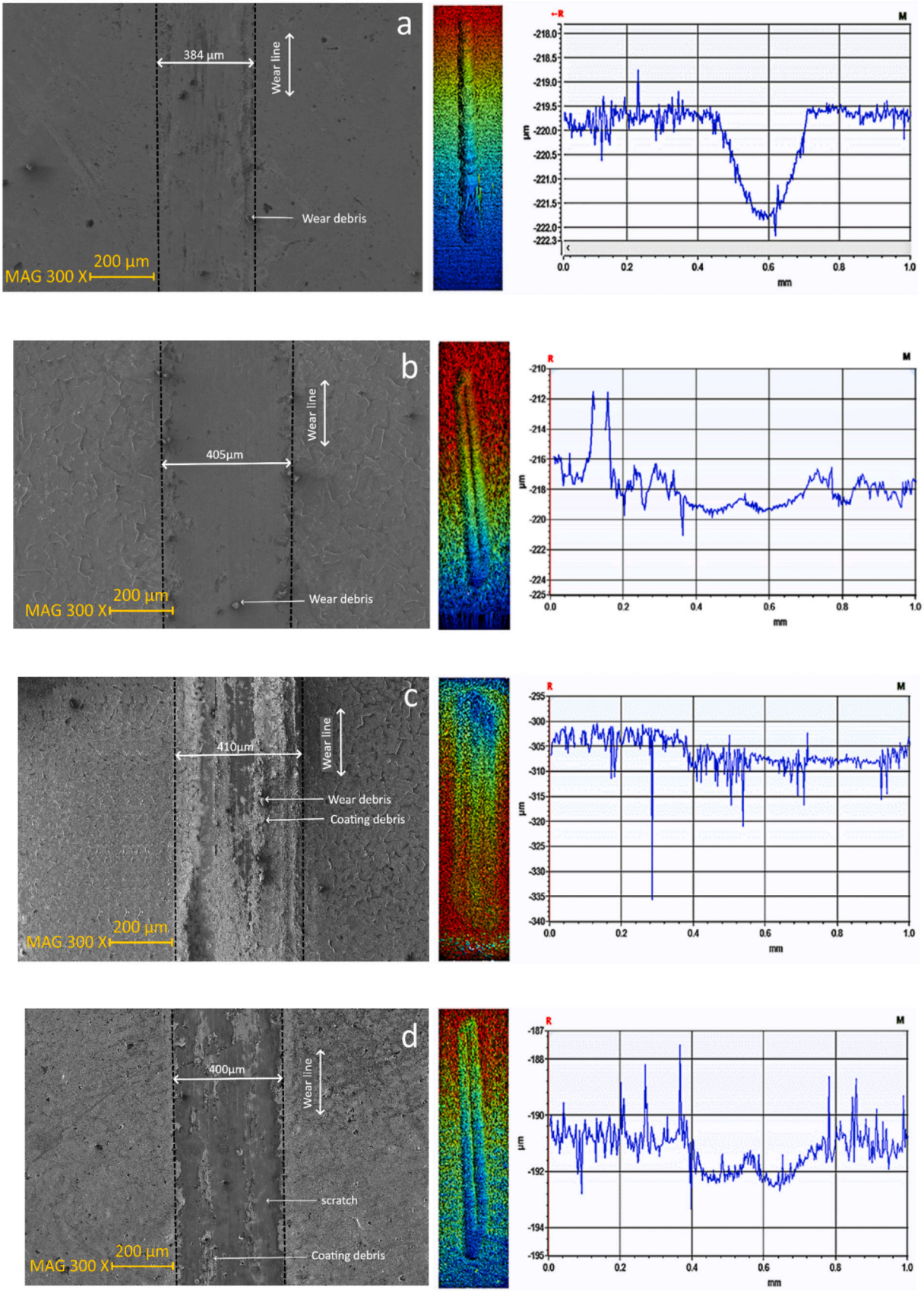


Fig. 7. Wear analysis during tribocorrosion of: a) unprocessed, b) Nitrided, c) Ti-DLC and d) duplex surface treated samples.

Table 4
Experimental findings of untreated and treated samples.

Sample	Layer thickness (μm)	Average surface roughness (Ra) (μm)	Average coefficient of friction	Wear rate (mm^3/Nm)
Untreated	–	0.06	0.78	4.38×10^{-6}
Nitrided	30–32	0.4	0.73	2.31×10^{-6}
Ti-DLC	5–7	0.08	0.52	1.84×10^{-6}
Duplex	35–37	0.32	0.77	6.50×10^{-7}

between the Fe, Cr and Ni in the stainless steel and Al_2O_3 causes the formation of wear products as wear continues and material transfer occurs from the soft AISI 316L stainless steel to the hard abrasive ball surface [27]. The presence of wear products formed between the ball and the sample transforms the wear mechanism from two-body wear to three-body wear [28]. It is thought that this transformation increases the wear rate, as the resulting transfer film has a stronger adhesion, which, as a result, causes more material to be separated from the sample surface. In the wear surface images, it was seen that untreated and nitrided 316L steel samples exhibited different wear behavior. Plate-shaped wear products were visible on the wear trace of the untreated sample. It may be stated that this situation occurred as a result of the plastic deformation of the transferred material or wear products during the wear test due to the frictional movement between the abrasive ball and the substrate. Wear products that harden by getting stuck between the abrasive ball and the sample, together with the sliding movement of the ball during wear, cause the formation of wear track on the 316L stainless steel surface. Another important point to note on the wear surfaces of the untreated 316L stainless steel sample was the excessive plastic deformation that occurred during wear. Plastic deformation signs were clearly visible from the wear scar depth. The increase in the imprint depth indicated that the soft stainless steel was deformed by the hard abrasive ball. Here, we can explain the wear behavior of the untreated sample as a combination of wear and plastic deformation mechanisms with severe adhesive wear. Plate-shaped wear products on the wear track are an indication of adhesive wear [29]. Thus, in the untreated sample (Fig. 7-a), the initially active mechanism was adhesive wear. Later, the effect of secondary particles and the scratches on the surfaces caused the abrasive wear process to be more effective. The wear behavior of the nitrided sample differed from that of the untreated sample. In the nitrided sample (Fig. 7-b), the coating on the surface eroded after a certain time and plastered towards the edges, causing adhesive wear due to the crushing of the surface. Particularly, the loss of particles for the coated samples decreased in liquid medium abrasions and it was determined that the friction created by the wear ball individually played a dominant role. The role of nitriding on the corrosion of 316L stainless steel is to counteract the plastic deformation of the specimen under load during wear and change the surface chemistry to reduce the likelihood of adhesion formation between the contacting surfaces. As a result of nitriding, the hardness increases from 2 to 5 times depending on the process conditions [5]. This increase in hardness is the most important reason for the decrease in the wear rate of nitrided samples. After the wear test, the wear trace depth of the nitrided sample decreased. When the wear trace on the nitrided surface was examined, it was observed that the wear generally occurred in the modified layer on the surface. Permanent deformations developed on the surfaces with the formation of adhesive wear on the surface treated samples. For this reason, it was seen that the abrasive wear mechanism was effective with the effect of adhesive and ceramic particles on the treated surfaces. Accordingly, it was determined that there was a decrease in the depth of the wear marks on the treated surfaces compared to the untreated sample at the beginning and with this reduction, the wear resistance of the treated samples increased in comparison to the untreated sample. It

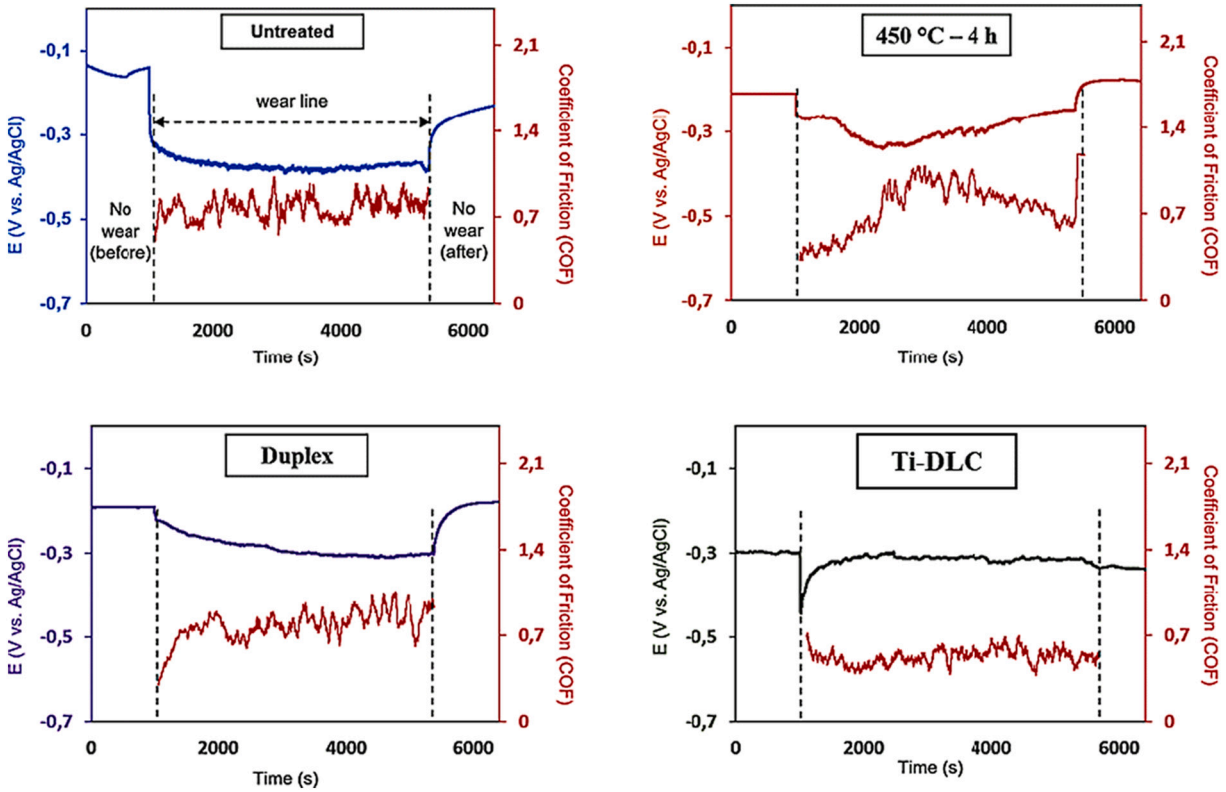


Fig. 8. Open circuit potential measurements and friction coefficient values during wear of untreated, nitrided, Ti-DLC coated and duplex treated samples in SBF solution.

was seen that the wear mechanism was cohesive in the Ti-DLC-coated and duplex surface-treated samples. In other words, the wear remained within the film (Fig. 7-a and Fig. 7-c). Here, the lowest wear trace depth value was seen in the samples with duplex surface treatment. On the wear marks, it was observed that the thin film decomposed in the form of spalling from place to place. The adhesion between the ball and the film caused the slip to occur between film and film as a result of material transfer from the film to the ball. It was observed that while some of the products that formed during wear were pushed towards the trace edges, some contributed to the transfer film by entrapping between the ball and the film in the shear direction [26]. Therefore, the best wear resistance was obtained in the duplex surface-treated samples. The hard and plastic deformation resistant nitride layer obtained before thin film coating increased the wear resistance of the duplex treated sample. Additionally, regardless of the coating type, it was seen that the wear marks reduced compared to the untreated sample. This meant that the coatings caused increased wear resistance.

In Table 4, the average friction coefficient (CoF) values of the samples obtained as a result of the experiments are given. The lowest coefficient of friction was measured as 0.52 in the direct Ti-DLC-coated sample. The friction coefficient of the duplex surface treated sample was higher than those of the Ti-DLC coated and plasma nitrided samples. The increased surface roughness as a result of nitriding, which is the first step of duplex surface treatment, caused the friction coefficient to be higher than the directly coated samples. It was observed that the friction coefficient did not change much over time and was stable in the coated and duplex surface-treated samples (Fig. 8). The friction coefficient increased rapidly at the beginning of the test. This was due to the fact that the upper points of the roughness on the sample surface first came into contact with the ball at the beginning of the friction test and the contact load was high but the surface area was very small. The friction coefficient value increases due to the Hertzian contact that occurs during this first contact and it then becomes stable with decreasing roughness as the contacting surfaces get settled with each other. Surface roughness is important in terms of friction and wear. In general, the friction coefficient increases as the surface roughness increases [30–33].

Tribocorrosion wear describes how materials interact and behave in this system between tribological and corrosion processes. Materials are exposed to mechanical, chemical and electrochemical processes in this system. Moreover, tribocorrosion carries uncertainty due to its chemical, electrochemical, physical and mechanical processes. In tribocorrosion tests, it is known that there is a connection between the wear volume and electrical charge transfer and higher wear is due to higher electrical transfer to the system during the test [34,35]. The coefficient of friction (CoF) values under the OCP conditions are given in Fig. 8. Here, the CoF values generally exhibited an unstable behavior. The cause of these local oscillations may have been related to the adhesion-sliding behavior between the sample and the Al_2O_3 ball and the formation and retention of new particles. During the OCP tests, the average CoF value for all samples varied between 0.52 and 0.78. A decrease in the COF value may occur due to the low roughness of the sample surface [36,37]. A steady state indicates the presence of a smoother contact surface [38]. In the SEM images in Fig. 7, it was observed that the plastic deformation effect of the wear mechanism was more dominant than the corrosive effects in the untreated sample. This effect could therefore produce delamination and wear residues on the wear surfaces. Since the hardness values of the coated samples were high, it was determined that these surfaces showed more resistance to wear. An increase in corrosive debris occurred on the hardened surfaces. This caused the formation of a third body on the surfaces [39,40]. In general, metal that is adhered to the surface will come into contact with the surface again during repeated sliding, causing further deformation. During this process, wear residues (third body particles) are formed due to cracking during the wear process (Fig. 7-c). While some of this debris is ejected from the contact area to the edges, causing wear loss, others remain in contact. Due to the adhesion forces, the debris is collected/compressed on the surface and forms new harder surface layers that can support the protection of the surface [41]. High wear rates were observed in the untreated samples. Therefore, grooves, cracks and corrosion attacks that occurred in these structures were more dangerous than other effects. In this case, the stick-slip event comes to the fore. For OCP conditions, wear marks will be wider than others. However, the reduction in the wear rates was measured the same for both conditions. Unstable plots were obtained due to the stick-slip behavior. It may be stated that the unstable structures that formed due to corrosion attacks affected the general hardness behavior of the coatings in the wear area. The thickness of the layer was found to be in direct proportion to nobility. Therefore, the duplex coating exhibited the best corrosion and friction resistance values.

In the SEM images given in Fig. 7, it is seen that the tribocorrosion resistance of the untreated sample was lower as a result of the tribocorrosion tests performed in the SBF solution. This situation occurred as a result of the low hardness and ionization energy level of the untreated sample and the wear in the sample quickly descended to the bottom in a short time with the onset of wear. As a result of the electrochemical effect and the onset of wear, the electrical potential applied to the sample also decreased. Since the untreated sample was in a relatively less aggressive environment in the SBF solution, it was properly abraded without fragmentation by the abrasive ball effect and exhibited a deep wear appearance, as seen in Fig. 7-a. Under the OCP conditions, no voltage was applied to the anodic region, and this region acted as a lubricant. Due to the de-passivation mechanism playing an active role in the untreated sample, the largest wear trace was formed and the tribocorrosion test resulted in a lower OCP value in this sample. A corrosive effect did not occur especially in the coated samples. Under the OCP conditions, the samples showed similar morphologies. It was determined that the thickness of the coating and diffusion zone was inversely proportional to the width of the wear trace. In other words, in this study, as the coating thickness increased, the hardness increased and the wear decreased. Therefore, the minimum wear rate was obtained in the duplex-coated samples in among all samples.

4. Conclusions

In this study, the tribocorrosion properties of untreated, plasma nitrided, Ti-DLC coated and duplex surface treated (Ti-DLC coating after nitriding) AISI 316L stainless-steel samples in a SBF solution were investigated. The results of the study can be summarized as follows:

- XRD results showed that a nitride layer consisting of s-phase formed after plasma nitriding. Also, it was seen that CrN phase did not form after plasma nitriding.
- Raman analyses showed that DLC films was successfully produced on both untreated and plasma nitrided samples.
- It was observed that the damage caused by the wear mechanism was much more severe than the damage caused by the corrosive effects.
- The best wear resistance was obtained in the duplex surface treated sample. Regardless of the coating type, it was determined that the wear marks were reduced compared to the untreated sample. This means that the coatings led to an increase in the wear resistance.
- During the OCP tests, the average COF values varied between 0.52 and 0.78. The thickness of the layer was found to be in direct proportion to nobility. Therefore, the duplex coating exhibited the best corrosion and friction resistance values.

CRediT authorship contribution statement

Y. Uzun: Conceptualization, Methodology, Validation, Investigation, Writing – original draft, Visualization, Supervision.

Declaration of competing interest

The authors declare that they have no known competing financial

interests or personal relationships that could have appeared to influence the work reported in this paper.

References

[1] L. Gil, S. Brühl, L. Jiménez, O. Leon, R. Guevara, M.H. Staia, Corrosion performance of the plasma nitrided 316L stainless steel, Surf. Coat. Technol. 201 (2006) 4424–4429, https://doi.org/10.1016/j.surfcoat.2006.08.081.

[2] A.F. Yetim, Investigation of wear behavior of titanium oxide films, produced by anodic oxidation, on commercially pure titanium in vacuum conditions, Surf. Coat. Technol. 205 (2010) 1757–1763, https://doi.org/10.1016/j.surfcoat.2010.08.079.

[3] H. Dong, S-phase surface engineering of Fe-Cr, Co-Cr and Ni-Cr alloys, Int. Mater. Rev. 55 (2010) 65–98, https://doi.org/10.1179/095066009X12572530170589.

[4] K.H. Lo, C.H. Shek, J.K.L. Lai, Recent developments in stainless steels, Mater. Sci. Eng. R. Rep. 65 (2009) 39–104, https://doi.org/10.1016/j.mser.2009.03.001.

[5] A.F. Yetim, M.Y. Codur, M. Yazici, Using of artificial neural network for the prediction of tribological properties of plasma nitrided 316L stainless steel, Mater. Lett. 158 (2015) 170–173, https://doi.org/10.1016/j.matlet.2015.06.015.

[6] H. Kovacı, Y.B. Bozkurt, A.F. Yetim, A. Çelik Baran, Corrosion and tribocorrosion properties of duplex surface treatments consisting of plasma nitriding and DLC coating, Tribol. Int. 156 (2021), 106823, https://doi.org/10.1016/j.triboint.2020.106823.

[7] M.T. Umemura, L.B. Varela, C.E. Pinedo, R.C. Cozza, A.P. Tschiptschin, Assessment of tribological properties of plasma nitrided 410S ferritic-martensitic stainless steels, Wear. 426–427 (2019) 49–58, https://doi.org/10.1016/j.wear.2018.12.092.

[8] E. Menthe, K.T. Rie, Further investigation of the structure and properties of austenitic stainless steel after plasma nitriding, Surf. Coat. Technol. 116–119 (1999) 199–204, https://doi.org/10.1016/S0257-8972(99)00085-7.

[9] C.P. Fenili, F.S. de Souza, G. Marin, S.M.H. Probst, C. Binder, A.N. Klein, Corrosion resistance of low-carbon steel modified by plasma nitriding and diamond-like carbon, Diam. Relat. Mater. 80 (2017) 153–161, https://doi.org/10.1016/j.diamond.2017.11.001.

[10] M. Jayalakshmi, P. Huilgol, B.R. Bhat, K.U. Bhat, Microstructural characterization of low temperature plasma-nitrided 316L stainless steel surface with prior severe shot peening, Mater. Des. 108 (2016) 448–454, https://doi.org/10.1016/j.matdes.2016.07.005.

[11] A.S. Hamdy, B. Marx, D. Butt, Corrosion behavior of nitride layer obtained on AISI 316L stainless steel via simple direct nitridation route at low temperature, Mater. Chem. Phys. 126 (2011) 507–514, https://doi.org/10.1016/j.matchemphys.2011.01.037.

[12] K. Farokhzadeh, A. Edrisy, Fatigue improvement in low temperature plasma nitrided Ti-6Al-4V alloy, Mater. Sci. Eng. A 620 (2015) 435–444, https://doi.org/10.1016/j.msea.2014.10.008.

[13] L. Trabzon, M.C. Iğdil, On the materials properties of thin film plasma-nitrided austenitic stainless steel, Surf. Coat. Technol. 200 (2006) 4195–4200, https://doi.org/10.1016/j.surfcoat.2004.12.012.

[14] C. Donnet, A. Erdemir, Tribology of Diamond-like Carbon Films: Fundamentals and Applications, Springer Science & Business Media, 2007.

[15] J. Robertson, Diamond-like amorphous carbon, Mater. Sci. Eng. R. Rep. 37 (2002) 129–281, https://doi.org/10.1016/s0927-796x(02)00005-0.

[16] B. Podgornik, J. Vizintin, H. Ronkainen, K. Holmberg, Friction and wear properties of DLC-coated plasma nitrided steel in unidirectional and reciprocating sliding, Thin Solid Films 377–378 (2000) 254–260, https://doi.org/10.1016/S0040-6090(00)01302-X.

[17] E.L. Dalibon, V. Trava-Airoldi, L.A. Pereira, A. Cabo, S.P. Brühl, Wear resistance of nitrided and DLC coated PH stainless steel, Surf. Coat. Technol. 255 (2014) 22–27, https://doi.org/10.1016/j.surfcoat.2013.11.004.

[18] E.I. Meletis, A. Erdemir, G.R. Fenske, Tribological characteristics of DLC films and duplex plasma nitriding/DLC coating treatments, Surf. Coat. Technol. 73 (1995) 39–45, https://doi.org/10.1016/0257-8972(94)02375-1.

[19] M.S. Jellesen, T.L. Christiansen, L.R. Hilbert, P. Møller, Erosion-corrosion and corrosion properties of DLC coated low temperature gas-nitrided austenitic stainless steel, Wear. 267 (2009) 1709–1714, https://doi.org/10.1016/j.wear.2009.06.038.

[20] M. Azzi, M. Paquette, J.A. Szpunar, J.E. Klemberg-Sapieha, L. Martinu, Tribocorrosion behaviour of DLC-coated 316L stainless steel, Wear. 267 (2009) 860–866, https://doi.org/10.1016/j.wear.2009.02.006.

[21] R. Bayón, A. Igartua, J.J. González, U. Ruiz De Gopegui, Influence of the carbon content on the corrosion and tribocorrosion performance of Ti-DLC coatings for biomedical alloys, Tribol. Int. 88 (2015) 115–125, https://doi.org/10.1016/j.triboint.2015.03.007.

[22] G.H. Zhao, R.E. Aune, N. Espallargas, Tribocorrosion studies of metallic biomaterials: the effect of plasma nitriding and DLC surface modifications, J. Mech. Behav. Biomed. Mater. 63 (2016) 100–114, https://doi.org/10.1016/j.jmbbm.2016.06.014.

[23] M. Łępicka, M. Grądzka-Dahlke, D. Pieniak, K. Pasierbiewicz, A. Niewczas, Effect of mechanical properties of substrate and coating on wear performance of TiN- or DLC-coated 316LVM stainless steel, Wear. 382–383 (2017) 62–70, https://doi.org/10.1016/j.wear.2017.04.017.

[24] F.H. ElBatal, G.T. El-Bassyouni, Bioactivity of Hench bioglass and corresponding glass-ceramic and the effect of transition metal oxides, Silicon. 3 (2011) 185–197, https://doi.org/10.1007/s12633-011-9095-6.

[25] A. Çelik, Y. Arslan, A.F. Yetim, I. Efeoglu, Fatigue behaviour of duplex treated AISI 316L stainless steel, Kov. Mater. 45 (2007) 35–40.

[26] Y. Liu, L. Liu, S. Li, R. Wang, P. Guo, A. Wang, P. Ke, Accelerated deterioration mechanism of 316L stainless steel in NaCl solution under the intermittent tribocorrosion process, J. Mater. Sci. Technol. (2022), https://doi.org/10.1016/j.jmst.2022.01.011.

[27] Y. Sun, T. Bell, Sliding wear characteristics of low temperature plasma nitrided 316 austenitic stainless steel, Wear. 218 (1998) 34–42, https://doi.org/10.1016/S0043-1648(98)00199-9.

[28] C.X. Li, T. Bell, Sliding wear properties of active screen plasma nitrided 316 austenitic stainless steel, Wear. 256 (2004) 1144–1152, https://doi.org/10.1016/j.wear.2003.07.006.

[29] A.F. Smith, The friction and sliding wear of unlubricated 316 stainless steel at room temperature in air, Wear. 96 (1984) 301–318, https://doi.org/10.1016/0043-1648(84)90043-7.

[30] A.F. Yetim, M. Yazici, Wear resistance and non-magnetic layer formation on 316l implant material with plasma nitriding, J. Bionic Eng. 11 (2014) 620–629, https://doi.org/10.1016/S1672-6529(14)60073-1.

[31] A.F. Yetim, A. Alsaran, A. Celik, I. Efeoglu, Corrosion behaviour of Ti DLC deposition on prenitrided 316L stainless steel and Ti-6Al-4V alloy, Corros. Eng. Sci. Technol. 46 (2011) 439–444, https://doi.org/10.1179/147842209X12464471864457.

[32] M. Yazici, O. Çomakli, T. Yetim, A.F. Yetim, A. Çelik, The effect of plasma nitriding temperature on the electrochemical and semiconducting properties of thin passive films formed on 316L stainless steel implant material in SBF solution, Surf. Coat. Technol. 261 (2015) 181–188, https://doi.org/10.1016/j.surfcoat.2014.11.037.

[33] I. Efeoglu, R.D. Arnell, S.F. Tinston, D.G. Teer, The mechanical and tribological properties of titanium aluminium nitride coatings formed in a four magnetron closed-field sputtering system, Surf. Coat. Technol. 57 (1993) 117–121, https://doi.org/10.1016/0257-8972(93)90027-L.

[34] E. Lemaire, M. Le Calvar, Evidence of tribocorrosion wear in pressurized water reactors, Wear 249 (2001) 338–344, https://doi.org/10.1016/S0043-1648(00)00544-5.

[35] L. Benea, P.L. Bonora, A. Borello, S. Martelli, Wear corrosion properties of nano-structured SiC-nickel composite coatings obtained by electroplating, Wear. 249 (2001) 995–1003, https://doi.org/10.1016/S0043-1648(01)00844-4.

[36] B. Bhushan, Introduction to Tribology, John Wiley & Sons, 2013.

[37] M. Buciumeanu, A. Bagheri, N. Shamsaei, S.M. Thompson, F.S. Silva, B. Henriques, Tribocorrosion behavior of additive manufactured Ti-6Al-4V biomedical alloy, Tribol. Int. 119 (2018) 381–388, https://doi.org/10.1016/j.triboint.2017.11.032.

[38] S. Kossman, L.B. Coelho, A. Mejias, A. Montagne, A. Van Gorp, T. Coorevits, M. Touzin, M. Poorteman, M.G. Olivier, A. Iost, M.H. Staia, Impact of industrially applied surface finishing processes on tribocorrosion performance of 316L stainless steel, Wear. 456–457 (2020), 203341, https://doi.org/10.1016/j.wear.2020.203341.

[39] F.H. Stott, High-temperature sliding wear of metals, Tribol. Int. 35 (2002) 489–495, https://doi.org/10.1016/S0301-679X(02)00041-5.

[40] S. Mischler, Triboelectrochemical techniques and interpretation methods in tribocorrosion: a comparative evaluation, Tribol. Int. 41 (2008) 573–583, https://doi.org/10.1016/j.triboint.2007.11.003.

[41] A. Bidiville, M. Favero, P. Stadelmann, S. Mischler, Effect of surface chemistry on the mechanical response of metals in sliding tribocorrosion systems, Wear. 263 (2007) 207–217, https://doi.org/10.1016/j.wear.2007.01.066.